

Integrating physical and genetic signals for programming across time scales in the mammalian cell.

Alexandre R. Sathler*

*UC Berkeley / UC San Francisco Joint Graduate Program in Bioengineering

Submitted to Principles of Synthetic Biology (Fall 2025)

Complex biological circuits and noisy environments necessitate robust signal delay machinery for connections across time scales. Here, I present TRAM: a synthesis of engineered protease cascades and cellular trafficking for a novel, tunable, hour-scale signal delay mechanism in mammalian cells. TRAM outperformed transcriptional gate matching in a temporal noise filtering task, highlighting its utility in broad synthetic biology applications.

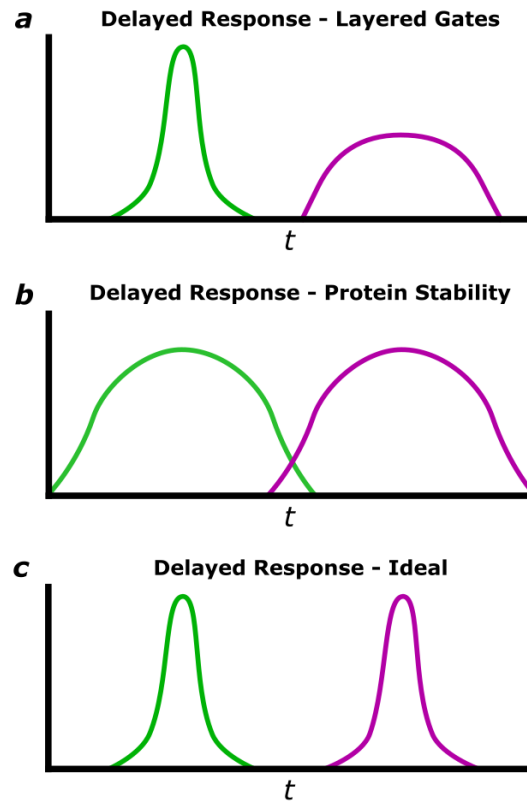
Trafficking | Protease Cascades | Signal Delays

1 Introduction

Despite increasingly tight control of signal response behavior in synthetic biological circuits (Brophy & Voigt, 2014), synthetic signal response delays present significant challenges. Traditionally, response delays are either engineered via nested transcriptional gating or altered protein stability.

Nested transcriptional gates provide broad design space for signal delays, but mismatched gate dynamic ranges combine with transcriptional stochasticity variability to attenuate output (Fig 1a). One alternative prolongs biological signals through physical persistence of signaling proteins (Weber et. al, 2007; Koh et. al, 2009; Wauford et. al, 2024), but utility is limited by the epigenetic silencing of long-lasting proteins in mammalian systems (Kim et. al, 2011). Persistent proteins also necessitate symmetrical ON and OFF kinetics: while long delays between ON and OFF signals may be achieved, signal periodicity is sacrificed (Fig. 1b).

Here, I model a novel delay mechanism combining protease cascades (Stein & Alexandrov, 2014; Yang et. al, 2025) with endogenous cellular transport machinery (TRAM) to achieve tunable stepwise delays between ON and OFF signals for idealized delays kinetics (Fig 1c.). To validate TRAM utility for synthetic biology, I demonstrate its superiority over traditional methods in producing a tunable, lightly attenuated output delay in response to pulsatile optogenetic stimulation.



2 TRAM Mechanism

As modeled, TRAM trafficking is induced by the addition of modular TRAM domains to a transcription factor (TF). Each TRAM domain consists of a nuclear localization sequence (NLS) and mitochondrial localization sequence (MTS) separated by an orthogonal protease cleavage site. The identity of the localization domain terminal to the transcription factor (NLS or MTS) induces trafficking and subsequent proteolytic cleavage (Fig 2).

To enable robust trafficking and cleavage, orthogonal TEV and TVMV proteases are constitutively expressed (Renna et. al, 2022), along with NLS or MTS ligand-binding sites at the membrane of respective sub-cellular organelles. Constitutive expression of these machinery leverages the endogenous mitochondrial outer-

membrane protein 20 (Tom20) membrane localization mechanism, where Tom20 transmembrane domains are recognized by mitochondrial inner-membrane protein 1 (Mim1) and inserted into the membrane.

After TF-TRAM construct expression, TF activity is delayed by sequential rounds of TRAM-mediated subcellular trafficking and TEV/TVMV-mediated proteolytic cleavage (Fig. 2a-c). The following is an example TF-TRAM construct with three TRAM domains:

TF-Ubr1-TVMV₁-NLS₁-TEV₁-MLS₁-TVMV₂-NLS₂-TEV₂-MLS₂-TVMV₃-NLS₃-TEV₃-MLS₃

The construct also contains Ubr1, a degron tag that ensures fast degradation (Varshavsky, 2019) upon TRAM domain exhaustion and TF localization to the nucleus (Fig. 2d).

3 Methods

I model TRAM delays as sequential trafficking between nucleus and mitochondria, with each cycle adding predictable delay and enabling sequential trafficking and proteolytic cleavage.

$$TFn_n \rightarrow TFn_m \rightarrow TFnC_m \rightarrow TFnC_n \rightarrow TF(n-1)_n \rightarrow \dots \rightarrow TF \quad (0)$$

To focus on circuit-level behavior as opposed to the complexities of biochemical implementation, I make four simplifying assumptions:

I. *Only the outermost cellular localization sequence is recognized.* Ensures sequential TRAM domain cleavage.

II. *Only the outermost protease cleavage site is accessible.* N-terminal protease cleavage sites are too distal from the protease for activity.

III. *The TF cannot enter the nucleus until all TRAM domains have been removed.* Ensures cleaves of all TRAM domains.

IV. *The Ubr1 domain is only active after all TRAM domains have been removed.* TF-TRAM construct persistence in the cytosol until all TRAM domains have been removed.

These principles save protein engineering and biochemical implementation for the future, allowing this work to focus on evaluating the merits of sub-cellular transcription factor trafficking for time delay circuits in synthetic biology.

3.1 Basic TRAM Model

I model TRAM delays as sequential trafficking between nucleus and mitochondria, with each cycle adding predictable delay and enabling sequential trafficking and proteolytic cleavage.

For definitions, see Supplementary Table 2. In compositor form, each trafficking and proteolytic processing step is converted into an ordinary differential equation (ODE):

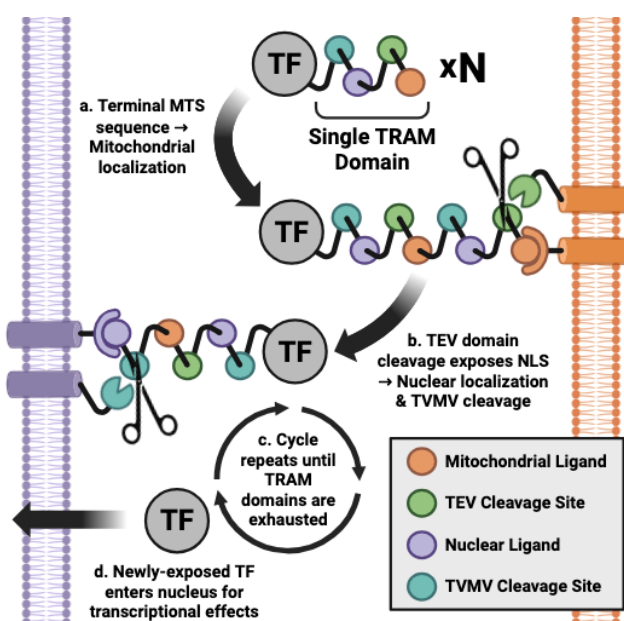


Figure 2: Schematic of TRAM Trafficking. TRAM is a tunable, physically separated sequential protease pathway. **a**, Terminal MTS sequences induce trafficking to the mitochondrial membrane, where MTS ligand-binding brings TF-TRAM constructs proximal to membrane-localized TEV protease **b**, TEV mediated proteolytic cleavage exposes NLS sequence (now terminal), inducing nuclear membrane trafficking. A mirrored NLS ligand-binding event localizes the TF-TRAM construct nearby to membrane-localized TVMV protease. **c**, TVMV mediated proteolytic cleavage reveals underlying TRAM domains if they are present, inducing another cycle of trafficking and TEV/TVMV cleavage. **d**, Upon exhaustion of all TRAM domains, the TF-Ubr1 construct is exposed and trafficked into the nucleus for transcriptional modulation and degradation.

$$\frac{dTFn_n}{dt} = k_{tx}PROM - \frac{V_a}{R_m}TFn_n - k_{dTR}TFn_n \quad (1.1)$$

$$\frac{dTFn_m}{dt} = \frac{V_a}{R_m}TFn_n - k_{TE}TFn_m - k_{dTR}TFn_m \quad (1.2)$$

$$\begin{aligned} \frac{dTFnC_m}{dt} &= k_{TE}TFn_m - \frac{V_a}{R_m}TFnC_m \\ &\quad - k_{dTR}TFnC_m \end{aligned} \quad (1.3)$$

$$\begin{aligned} \frac{dTFnC_n}{dt} &= \frac{V_a}{R_m}TFnC_m - k_{TV}TFnC_n \\ &\quad - k_{dTR}TFnC_n \end{aligned} \quad (1.4)$$

$$\begin{aligned} \frac{dTF(n-1)_n}{dt} &= k_{TV}TFnC_n - \frac{V_a}{R_m}TF(n-1)_n \\ &\quad - k_{dTR}TF(n-1)_n \end{aligned} \quad (2.1)$$

...

$$\frac{dT}{dt} = k_{TV}TF1C_n - k_{dTF}TF1C_n \quad (N.4)$$

The fifth equation was written to illustrate the cyclical nature of the described ODE system: when the final TRAM domain component is cleaved from the previous cycle, the next cycle begins. The last equation depicts the ultimate step where the final TRAM domain is cleaved and TF-Ubr1 simultaneously becomes transcriptionally active and open to Ubr1-mediated proteolysis.

3.2 Input Pulse Modeling

Input pulses were modeled as a gaussian distribution of protein production. The equation used for the magnitude (M) of transcriptional activity at time t along the gaussian curve was as follows:

$$M = A \cdot e^{-\frac{1}{2}(\frac{t-t_p}{w})^2} \quad (3.2)$$

A is the maximum amplitude of the transcriptional activity, t_p is the time at which peak production is achieved, and w corresponds to the width of the peak. Supp. Table 3 contains parameter values for various pulse types used in this work.

3.3 Solving ODEs

ODEs were solved in python (v3.13.7) using `solve_ivp` from the Scipy package (v1.16.1). Unless otherwise stated, the RK45 solving method was used to simulate TF-TRAM-mediate output pulse delays over 24 hours with a timestep (Δt) of one second.

3.4 TRAM Parameter Sensitivity Modeling

Optogenetic pulse parameters V_a , k_{TEV} , k_{dTR} , and k_{dTF} were linearly transformed in by multiples of two. Each parameter was transformed by multiples in a range from 1/6x to 6x, yielding 2401 combinations of the four parameters. All combinations were solved as in Section 3.3 via a model system containing TF-6xTRAM construct stimulated by an optogenetic pulse (Supp. Table 3). In simulations, k_{TEV} and k_{TVMV} were due to mechanistic similarity.

3.5 Code Availability

All code and associated documentation can be found at this work's GitHub repository: https://github.com/AlexSath/PoSB_Fall_2025_Final_Project.

4 Results

4.1 Short input pulses are required for scale-appropriate TRAM delays.

TF-TRAM construct with four TRAM domains (TF-4xTRAM) was modeled using empirically-measured system parameters (Supp. Table 1). A TF-4xTRAM construct was transcribed for three hours (CITATION), and output TF concentrations were graphed with respect to time. While output expression (REU) was delayed, its timing was indistinguishable from that of trafficking intermediates, suggesting that any delay observed resulted from transcriptional dynamics as opposed to TRAM trafficking (Fig. 1a).

I then wondered whether a shorter TF-TRAM transcriptional pulse would resolve incremental time delays associated with trafficking of individual TRAM domains. I modeled a six-minute, optogenetically-induced pulse (CITATION) of transcriptional activity of the same TF-4xTRAM construct. Output TF expression was delayed relative to the initial pulse and residual expression of TRAM intermediates were resolved (Fig. 1b) unlike the transcriptional pulse.

4.2 Output signal delays scale linearly with TRAM domain count.

To investigate whether incrementally appending TRAM domains to the TF-TRAM peptide would incrementally increase output signal delays, between one and eight TRAM domains were modeled. Each additional TRAM domain incrementally

increased output delays when initially induced by an optogenetic pulse (Fig. 1c); furthermore, regression analysis produced a linear fit to increasing time delays (Fig. 1d). A logarithmic fit of output peak REU indicated that additional TRAM domains also attenuate signal (Fig. 1e), likely due to protein degradation in the cytosol. These results suggest that each additional TRAM domain adds 140 seconds of delay between input and output signals under literature-informed conditions.

4.3 TF-TRAM trafficking speed post optogenetic stimulation does not prolong delays.

To assay system robustness in the face of diverse modeling parameters, linear transformations were made to trafficking time, proteolytic activity, TF-TRAM persistence in the cytoplasm, and TF persistence in the nucleus.

While both cell diameter and trafficking speed would linearly modify trafficking time, trafficking speed was selected because it is more flexible: cell diameter is difficult to change in a cell type, but trafficking speed can be modified positively via active transport or negatively via rate-limiting steps

such as membrane insertion. Contrary to a trafficking-based delay hypothesis, perturbations to TF-TRAM cytoplasmic trafficking speed (V_a) had no effect on pulse output or amplitude (Fig. 4a).

Linear transformation of TF-TRAM construct persistence in the cytoplasm via degradation rates (k_{dTR}) also yielded no change to output delay or amplitude (Fig. 2c); however, it is unlikely this would hold true for longer, non-optogenetic input pulses.

4.4 Proteolytic activity and TF degradation rates modulate optogenetic delays.

Linear transformation of proteolysis kinetics (k_{TEV}) revealed a logarithmic decrease in output signal delays with increasing proteolytic activity (Fig. 2b). Increased proteolytic activity also yielded a milder, loosely sigmoidal increase in peak output expression. Together, these results suggest that k_{TEV} remains the rate-limiting step for intermediate trafficking despite time-constrained optogenetic pulse inputs.

While perturbations to transcription factor degradation rates (k_{dTf}) had little effect on signal output

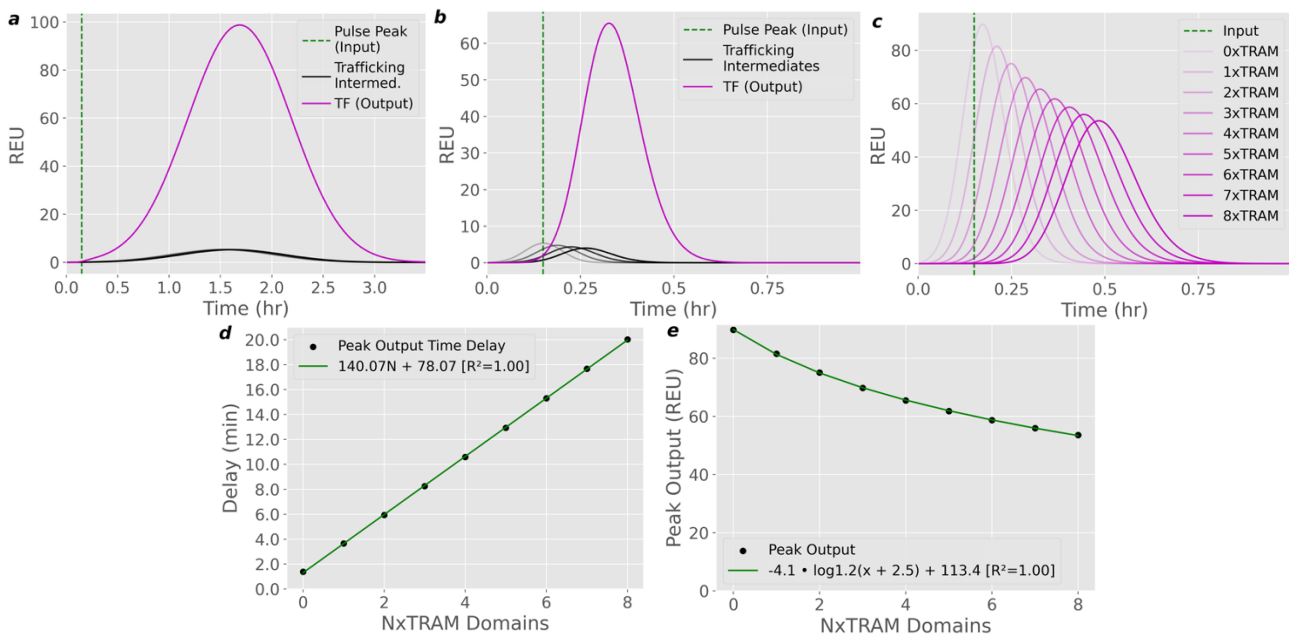


Figure 3 | Effect of Pulse Duration and TRAM Domains on Output Delay. Depictions of output signal peaks based on a simulated TF-TRAM system. **a**, Model with parameters rigidly faithful to biological plausibility, TF-4xTRAM output signal is significantly delayed from peak input signal, but intermediate trafficking is not resolved. **b**, A short optogenetic pulse resolves TRAM intermediates in the TF-4xTRAM construct. **c**, Incremental addition of TRAM domains to TF-TRAM construct increases output time delay. **d**, Signal delay scales linearly with TRAM domain count. **e**, Output signal amplitude decreases logarithmically with increasing TRAM domain count.

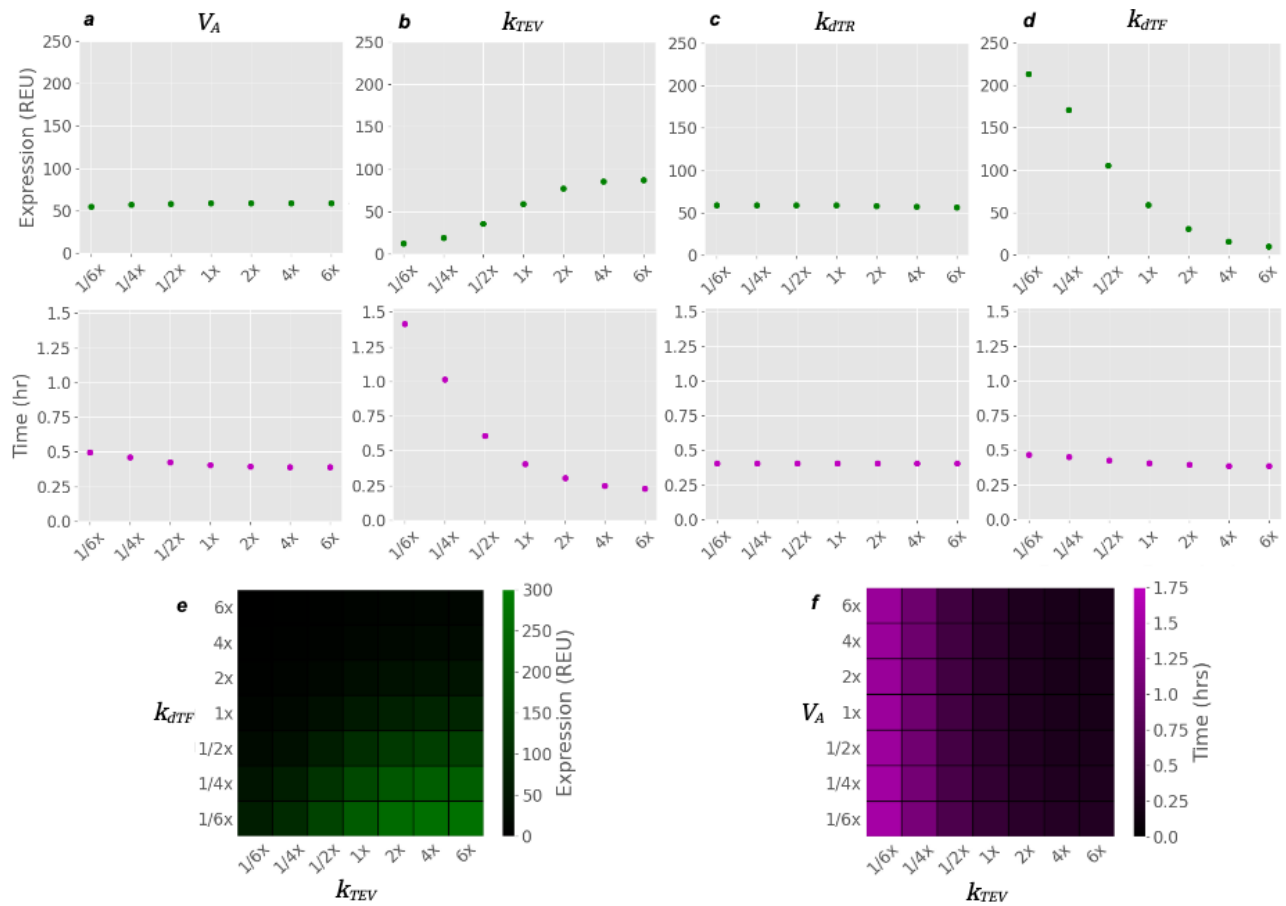
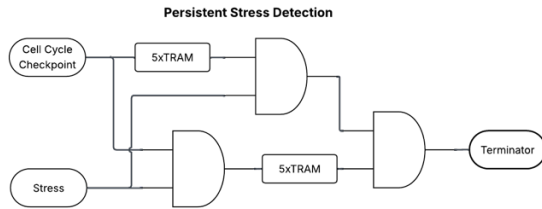


Figure 4 | Delay time and amplitude in system parameter space. Output transcriptional activity was modeled with a TF-6xTRAM construct and an optogenetic pulse (Supp. Table 3). **a**, Fold changes in transport velocity (V_A) have no effect on output pulse amplitude and minor effects on output pulse delay. **b**, Output pulse amplitude shows sigmoidal response to fold changes in protease catalytic rate (k_{TEV}), while output pulse delay decreases logarithmically. **c**, Fold changes to cytosolic TF-TRAM degradation rate (k_{dTR}) have no effect on output pulse amplitude or delay. **d**, Output pulse amplitude decreases logarithmically in response to increasing fold changes to post-TRAM TF-Ubr1 degradation rate (k_{dTF}). **e**, Combination 6-fold decrease in k_{dTF} and 6-fold increase in k_{TEV} produced the highest output amplitude. **f**, Six-fold decrease in k_{TEV} contributed significantly and six-fold decrease in V_A contributed slightly to highest modeled TRAM delay.

delays, increasing k_{dTF} resulted in logarithmic decreases of peak output expression.

6 TRAM vs. Gate Layering in Synthetic Circuits



7 Discussion

Logarithmic increase of k_{tev} -mediated signal delay with decreasing k_{tev} suggests reducing proteolysis rates would be a robust way to increase wait times. While this peak output amplitude would be reduced, this could be rescued by a proportional decrease in transcription factor degradation rates (k_{dTF}) (Fig. 4e). Protein engineering therefore makes k_{tev} a reasonable delay mechanism for both optogenetic and transcriptional pulses.

Trafficking velocity (V_a) has little effect on signal delays relative to k_{TEV} , but could be a useful engineering tactic for delaying optogenetic pulse outputs in specialized cell types where distances are large, such as neurons.

This analysis could be changed by a trafficking-mediated rate-limiting step, such as cargo binding to motor proteins, but that was out of the scope of this study.

Further experimentation: sigmoidal response curve with k_{TEV} vs. peak output expression?

Further experimentation: discuss lack of output signal width analysis, which would likely reveal a significant downside to increased peak output expression with decreased k_{dTF} (Fig. 4d).

8 Citations

Brophy, J., Voigt, C. Principles of genetic circuit design. *Nat Methods* **11**, 508–520 (2014). [doi](#).

Das, S., Vera, M., Gandin, V., Singer R.H., Tutucci E. Intracellular mRNA transport and localized

translation. *Nature Reviews Molecular & Cell Biology* **22**, 483–504 (2021). [Doi](#).

Hulett, J.M., Lueder, F., Chan, N.C., Perry, A.J., Wolynec, P., Likić, V.A., Gooley, P.R., Lithgow, T. The transmembrane segment of Tom20 is recognized by Mim1 for docking to the mitochondrial TOM complex. *J Mol Biol.* **376**(3), 694-704 (2008). [doi](#).

Kim, M., O'Callaghan, P. M., Droms, K. A. & James, D. C. A mechanistic understanding of production instability in CHO cell lines expressing recombinant monoclonal antibodies. *Biotechnol. Bioeng.* **108**, 2434–2446 (2011). [doi](#).

Koh, K.W., Lehming, N., Seah, G.T. Degradation-resistant protein domains limit host cell processing and immune detection of mycobacteria. *Mol Immunol* **46**, 1312-1318 (2009). [doi](#).

Li, J., Wu, F., Cheng, L., Zhang, J., Cha, C., Chen, L., Feng, T., Zhang, J., Guo, G. A nuclear localization signal is required for the nuclear translocation of Fign and its microtubule-severing function. *Mol Med Rep.* **21**(6), 2367-2374 (2020). [doi](#).

Renna, P., Ripoli, C., Dagliyan, O., Pastore, F., Rinaudo, M., Re, A., Paciello, F., Grassi, C. Engineering a switchable single-chain TEV protease to control protein maturation in living neurons. *Bioeng Transl Med.* **7**(2), e10292 (2022). [doi](#).

Stein, V., Alexandrov, K. Protease-based synthetic sensing and signal amplification, *Proc. Natl. Acad. Sci. U.S.A.* **111** (45), 15934-15939 (2014). [doi](#).

Varshavsky, A. N-degron and C-degron pathways of protein degradation, *Proc. Natl. Acad. Sci. U.S.A.* **116** (2) 358-366 (2019). [doi](#).

Wauford, N., Wachter, G., Kiwimagi, K., Weiss, R. A Tunable Long Duration Pulse Generation Circuit in Mammalian Cells. *ACS Synthetic Biology* **13**, 11, 3576–3586 (2024). [doi](#).

Weber, W., Stelling, J., Rimann, M., Keller, B., Daoud-El Baba, M., Weber, C.C., Aubel, D., Fussenegger, M. A synthetic time-delay circuit in mammalian cells and mice, *Proc. Natl. Acad. Sci. U.S.A.* **104** (8) 2643-2648 (2007). [doi](#).

Yang, H.K., Muthukumar, P.K., Chen, W. Synthetic protein degradation circuits using programmable cleavage and ligation by Sortase A. *Nat Commun.* **16**(1), 8682 (2025). [doi](#).

9 Supplemental Information

Table 1: Biophysical modeling parameters		
Variable	Description	Value
V_a	Velocity of motor protein trafficking	0.47 μm/s
k_{TEV}/k_{TVMV}	Rate of proteolytic activity	0.015/s
k_{dTR}	Rate of cytoplasmic degradation of TF-TRAM constructs	1x10 ⁻⁵ /s
k_{dTf}	Rate TF-Ubr1 degradation post TRAM domain exhaustion	0.01
V_d	Linear diffusion coefficient in cytoplasm	27 μm ² /s
R_n	Mean radius of the nucleus	2.5 μm
R_c	Mean radius of a cell	7.5 μm
R_m	Mean nucleus-mitochondria distance	2.5 μm

Table 2: Parts in a single TRAM trafficking cycle	
Variable	Description
TFn_n	TF with n TRAM domains localized at the nucleus.
TFn_m	TF with n TRAM domains localized at the mitochondria.
$TFnC_m$	TF with n TRAM domains localized at the mitochondria, after TEV cleavage.
$TFnC_n$	TF with n TRAM, post-TEV cleavage, re-localized to the nucleus.
$TF(n-1)_n$	TF, post-TVMV cleavage, now containing $n-1$ TRAM domains
TF	TF-Ubr1 free of TRAM domains that traffics to nucleus for transcriptional modulation and degradation

Table 3: Gaussian Pulse Parameters			
Variable	Transcriptional	Phosphorylation	Optogenetic
A (REU/s)	1	1	1
t_p (s)	5400	1350	540
w (s)	1800	675	180